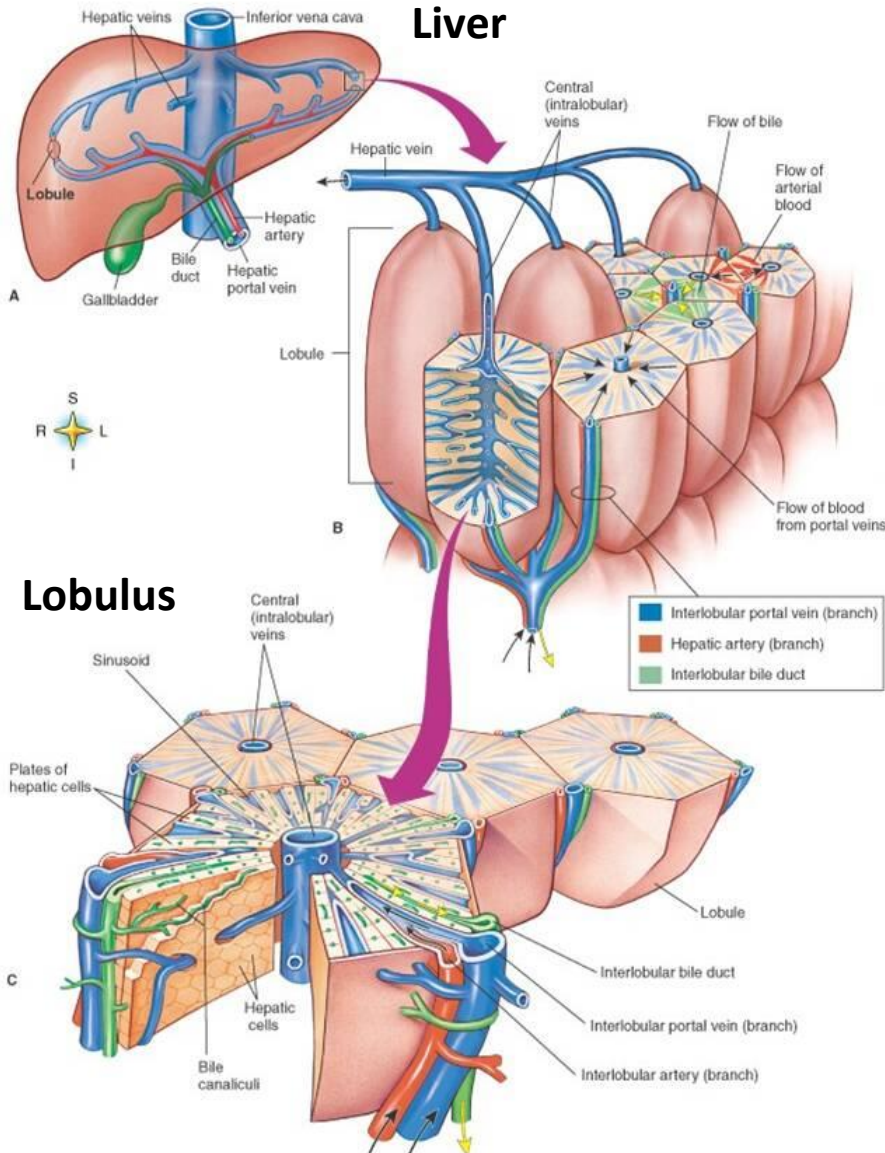
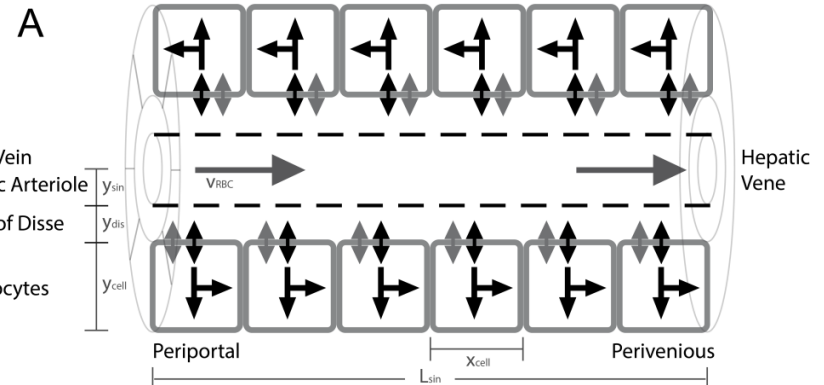


LIVER ARCHITECTURE



- liver structured in parallel subunits (**liver lobule**)
- liver lobulus consists of **network of sinusoids** connecting hepatic artery and portal vein with the **central vein (periportal → perivenous)**
- **Sinusoidal Unit** consists of central sinusoid surrounded by hepatocytes separated by the space of Disse

Sinusoidal Unit



CELLULAR SCALE - HEPATOCYTES

- liver most important organ for whole-body metabolism and clearance of galactose

- Main enzymatic steps

- I. **Galactokinase (GALK)**
phosphorylation of galactose (gal) to galactose 1-phosphate (gal1p) catalysed
- II. **Galactose-1-phosphate uridyl transferase (GALT)**
conversion of gal1p to UDP-galactose (udpgal)
- III. **UDP-galactose 4'-epimerase (GALE)**
interconversion of udpgal and UDP-glucose (udpglc)

-

Metabolites: (adp) **ADP**; (atp) **ATP**; (gal) **D-galactose**; (gal1p) **D-galactose 1-phosphate**; (galnat) **D-galactonate**; (galtol) **D-galactitol**; (glc) **D-glucose**; (glc1p) **D-glucose 1-phosphate**; (glc6p) **D-glucose 6-phosphate**; (nadp) **NADP**; (nadph) **NADPH**; (pi) **phosphate**; (pp) **pyrophosphate**; (udp) **UDP**; (udpgal) **UDP-D-galactose**; (udpglc) **UDP-D-glucose**; (utp) **UTP**;

GALACTOSEMIAS

Table 4 - Kinetic parameters in GALK, GALT and GALE deficiencies.

- caused by **deficiencies in either GALK, GALT or GALE**
- untreated as well as treated patients with galactosemia show accumulation and/or depletion of specific metabolites, and often abnormalities of glycosylation

implementation

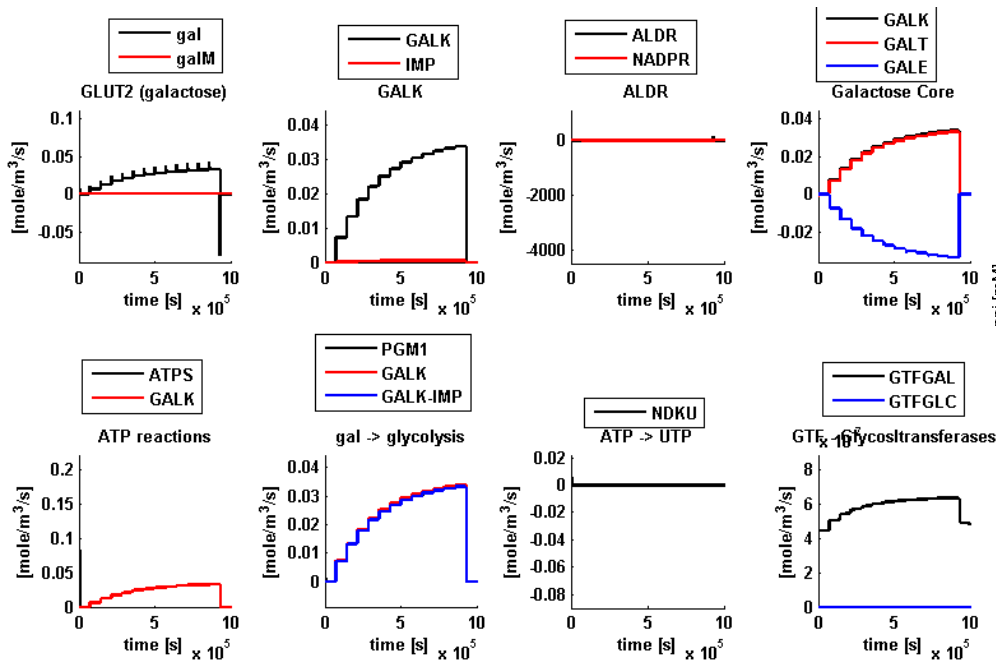
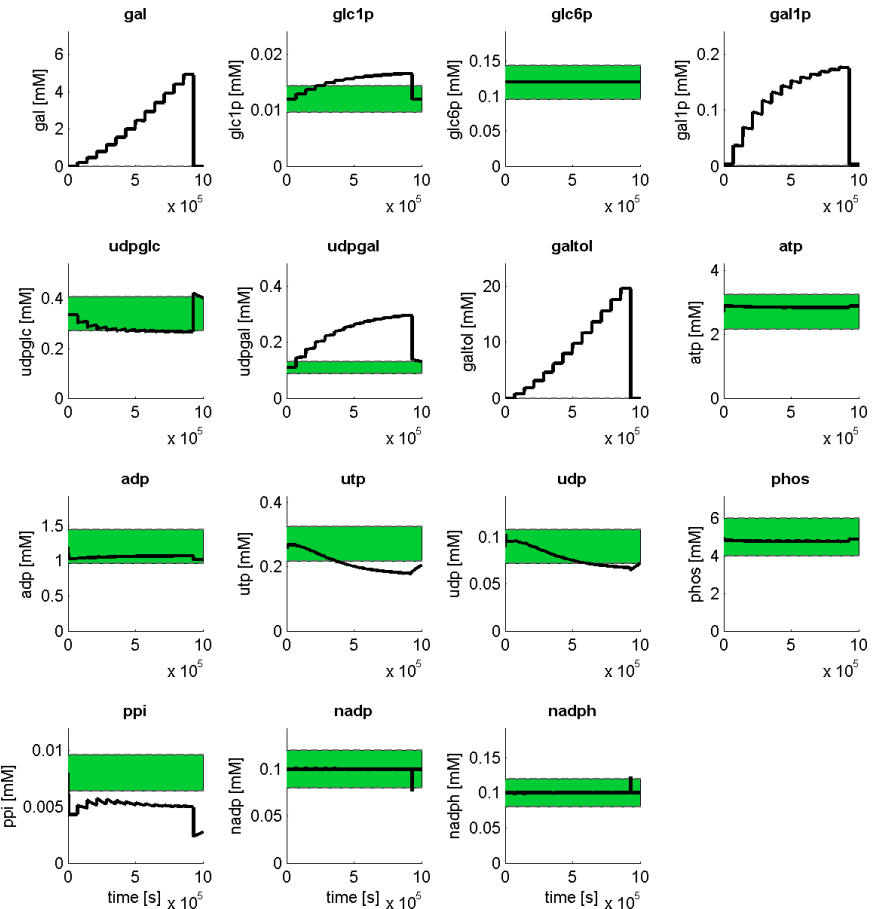
- via measured alterations in kinetic properties in human protein mutations

	Enzyme	Variant	k_{cat} [1/s] (%wt)	$K_m(gal)$ [mM] (%wt)	$K_m(atp)$ [mM] (%wt)	Reference
	GALK	Wild Type	8.7±0.5 (100)	0.97±0.22 (100)	0.034±0.004 (100)	[51]
1	GALK	H44Y	2.0±0.1 (23)	7.70±4.40 (794)	0.130±0.009 (382)	[51]
2	GALK	R68C	3.9±0.8 (45)	0.43±0.15 (44)	0.110±0.035 (324)	[51]
3	GALK	A198V	5.9±0.1 (68)	0.66±0.22 (68)	0.026±0.001 (76)	[51]
4	GALK	G346S	0.4±0.04 (5)	1.10±0.16 (113)	0.005±0.002 (15)	[51]
5	GALK	G347S	1.1±0.2 (13)	13.0±2.0 (1340)	0.089±0.034 (262)	[51]
6	GALK	G349S	1.8±0.1 (21)	1.70±0.48 (175)	0.039±0.004 (115)	[51]
7	GALK	E43A	6.7±0.02 (77)	1.90±0.50 (196)	0.035±0.0003 (103)	[100]
8	GALK	E43G	0.9±0.02 (10)	0.14±0.01 (14)	0.0039±0.0006 (11)	[100]
	Enzyme	Variant	V_{max} [nmol/mg/s] (% wt)	$K_m(gal1p)$ [mM] (%wt)	$K_m(udp1p)$ [mM] (%wt)	Reference
	GALT	Wild Type	804±65 (100)	1.25±0.36 (100)	0.43±0.09 (100)	[22]
9	GALT	R201C	396±59 (49)	1.89±0.62 (151)	0.58±0.13 (135)	[22]
10	GALT	E220K	253±53 (31)	2.34±0.42 (187)	0.69±0.16 (160)	[22]
11	GALT	R223S	297±25 (37)	1.12±0.31 (90)	0.76±0.09 (177)	[22]
12	GALT	I278N	45±3 (6)	1.98±0.35 (158)	1.23±0.28 (286)	[22]
13	GALT	L289F	306±23 (38)	2.14±0.21 (171)	0.48±0.13 (112)	[22]
14	GALT	E291V	385±18 (48)	2.68±0.16 (214)	0.95±0.43 (221)	[22]
	Enzyme	Variant	k_{cat} [1/s] (%wt)	$K_m(udp1p)$ [mM] (%wt)		Reference
	GALE	Wild Type	36±1.4 (100)	0.069±0.012 (100)		[59]
15	GALE	N34S	32±1.3 (89)	0.082±0.015 (119)		[59]
16	GALE	G90E	0.046±0.0028 (0)	0.093±0.024 (135)		[59]
17	GALE	V94M	1.1±0.088 (3)	0.160±0.038 (232)		[59]
18	GALE	D103G	5.0±0.23 (14)	0.140±0.021 (203)		[59]
19	GALE	L183P	11±1.2 (31)	0.097±0.040 (141)		[59]
20	GALE	K257R	5.1±0.29 (14)	0.066±0.015 (96)		[59]
21	GALE	L313M	5.8±0.36 (16)	0.035±0.011 (51)		[59]
22	GALE	G319E	30±1.3 (83)	0.078±0.013 (113)		[59]
23	GALE	R335H	15±0.48 (42)	0.099±0.012 (143)		[59]

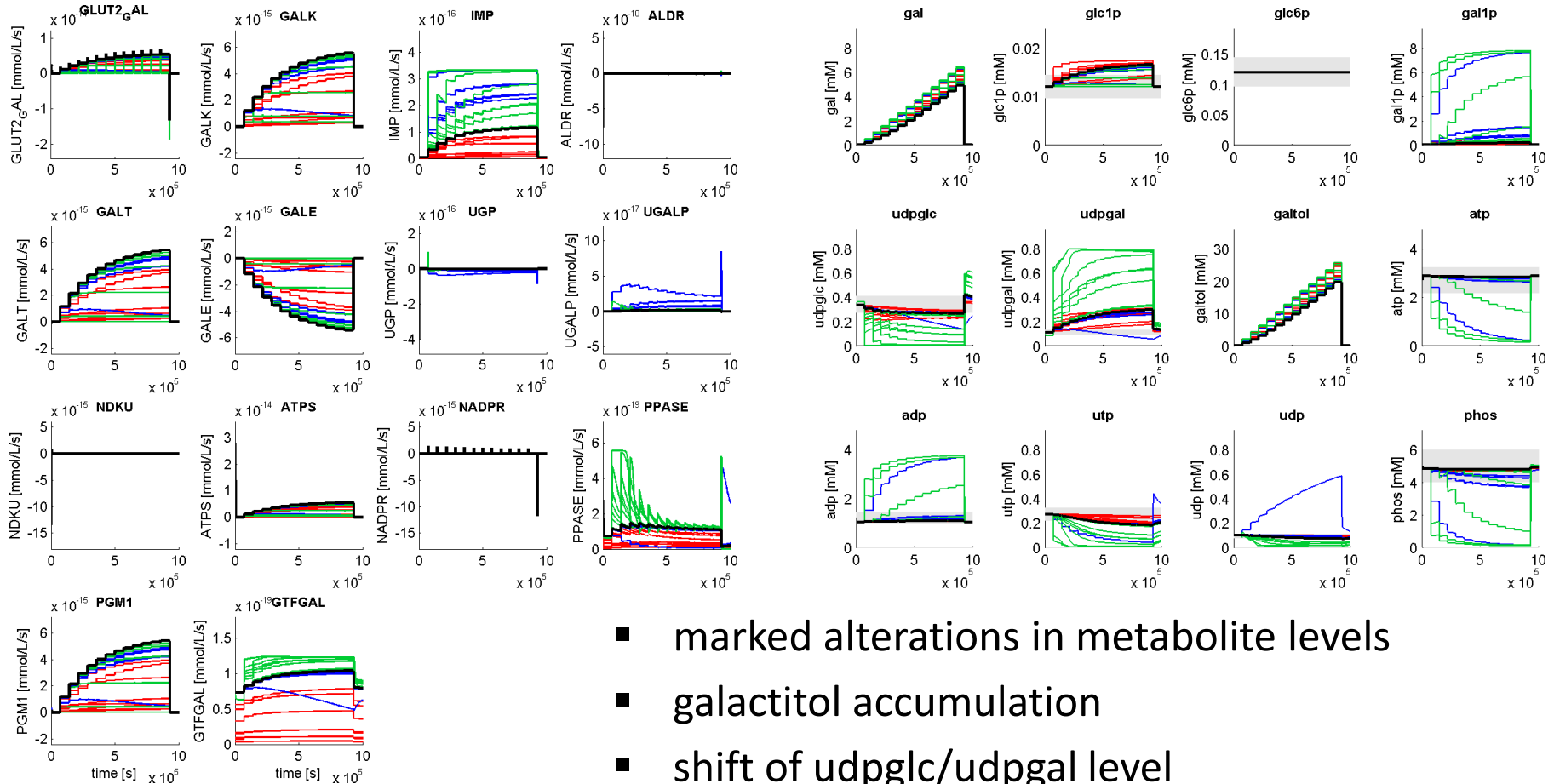
HEPATOCYTE MODEL

■ Reproduces

- metabolic concentrations normal state
- altered metabolite levels during galactose challenge
- saturation of clearance capacity



GALACTOSEMIA (GALK, GALT, GALE)

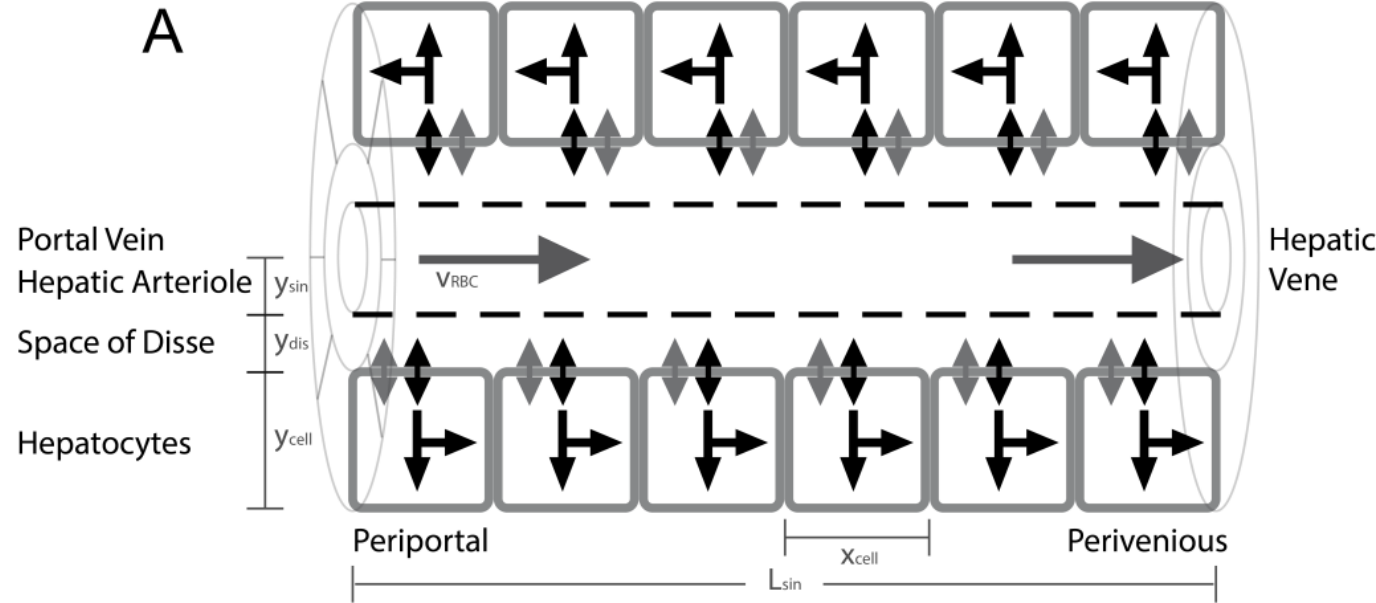


- marked alterations in metabolite levels
- galactitol accumulation
- shift of udpglc/udpgal level
- reduced galactose clearance
- energetically challenged

**TISSUE-SCALE –
SINUSOIDAL UNIT**

TISSUE-SCALE: SINUSOIDAL UNIT

Parameter	Symbol	Model
Tisse/Cell scale		
number of hepatocytes along sinusoid	N_c	20
discretization space of Disse and sinusoid per cell	N_f	5
sinusoid length	L_{sin}	500 μ m
diameter hepatocytes in direction sinusoid	x_{cell}	L_{sin} / N_c (25 μ m)
discretization along sinusoids	x_{sin}	x_{cell} / N_f (5 μ m)
sinusoidal radius	y_{sin}	4.4 μ m



Area between adjacent sinusoid compartments	A_{sin}	$\pi(y_{sin})^2$
Area between adjacent Disse compartments	A_{dis}	$\pi(y_{sin} + y_{dis})^2 - A_{sin}$
Area between adjacent sinusoid and Disse compartments	$A_{sin dis}$	$2\pi \cdot y_{sin} \cdot x_{sin}$
Volume sinusoid compartment	V_{sin}	$A_{sin} \cdot x_{sin}$
Volume Disse compartment	V_{dis}	$A_{dis} \cdot x_{sin}$
Volume cell	V_{cell}	$\pi((y_{sin} + y_{dis} + y)^2 + (y_{sin} + y_{dis})^2) \cdot x_{cell}$

Blood flow in sinusoid

$$v_{sin,flow}^{pp \rightarrow k=1} = v_{blood} A_{sin} x_{pp} \left[\frac{mole}{s} \right] \quad (x_{pp} \rightarrow x_{sin}^1)$$

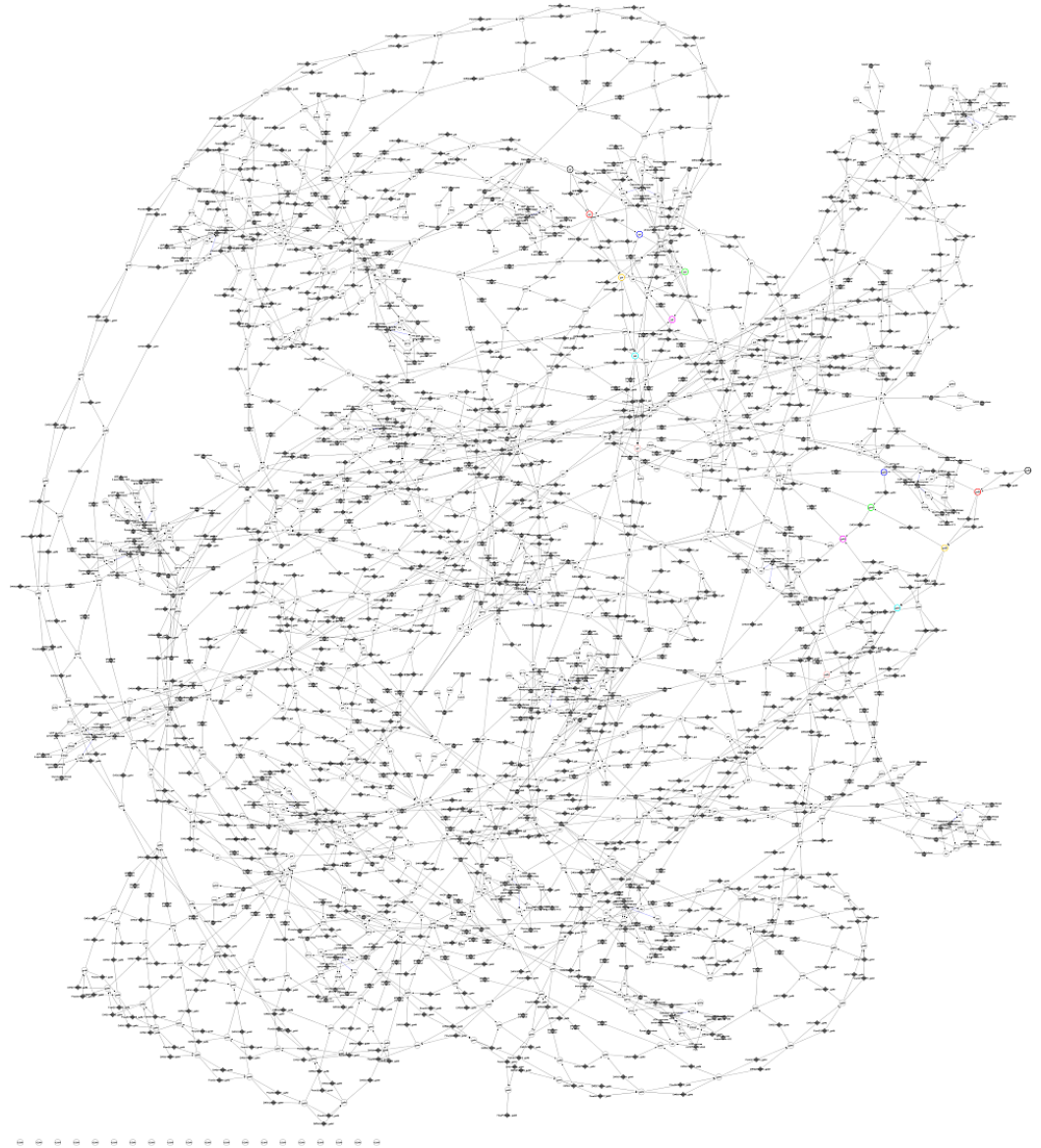
$$v_{sin,flow}^{k \rightarrow k+1} = v_{blood} A_{sin} x_{sin}^k \left[\frac{mole}{s} \right] \quad (x_{sin}^k \rightarrow x_{sin}^{k+1})$$

$$v_{sin,flow}^{k=N_b \rightarrow pv} = v_{blood} A_{sin} x_{sin}^{k=N_b} \left[\frac{mole}{s} \right] \quad (x_{sin}^{N_b} \rightarrow x_{pv})$$

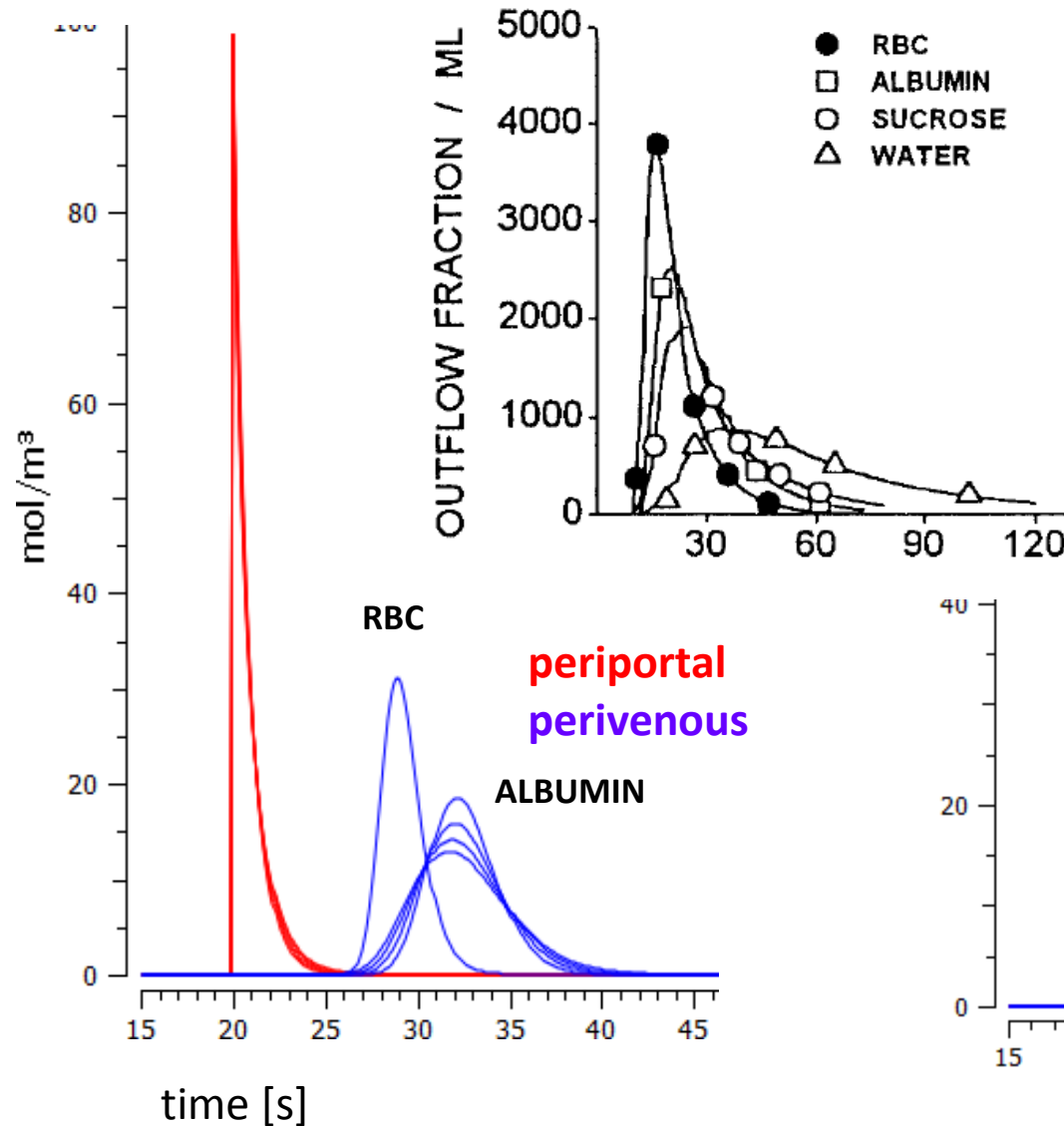
$$v_{sin,flow}^{pv \rightarrow} = v_{blood} A_{sin} x_{pv} \left[\frac{mole}{s} \right] \quad (x_{pv} \rightarrow)$$

MODEL HAIRBALL

- ~4000 species & ~4000 reactions

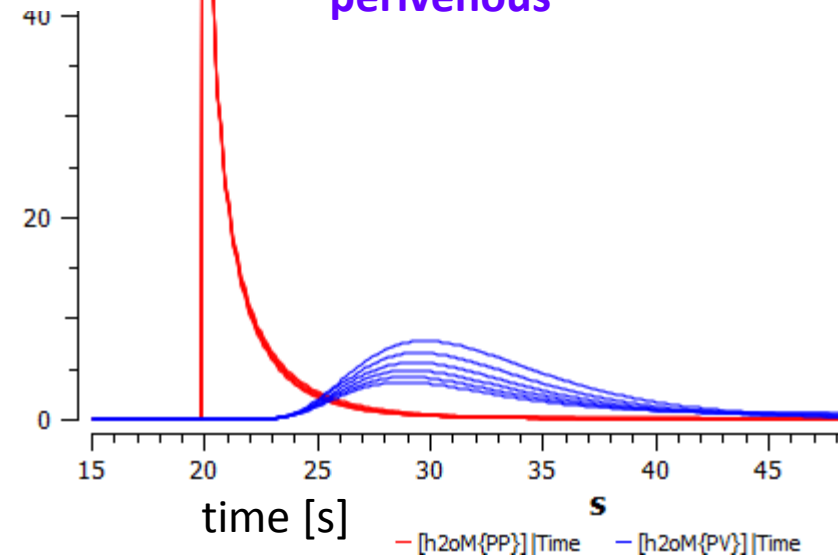


MULTIPLE-INDICATOR DILUTION SIMULATION



WATER: varying exchange rates with hepatocytes

periportal
perivenous



WORK IN PROGRESS

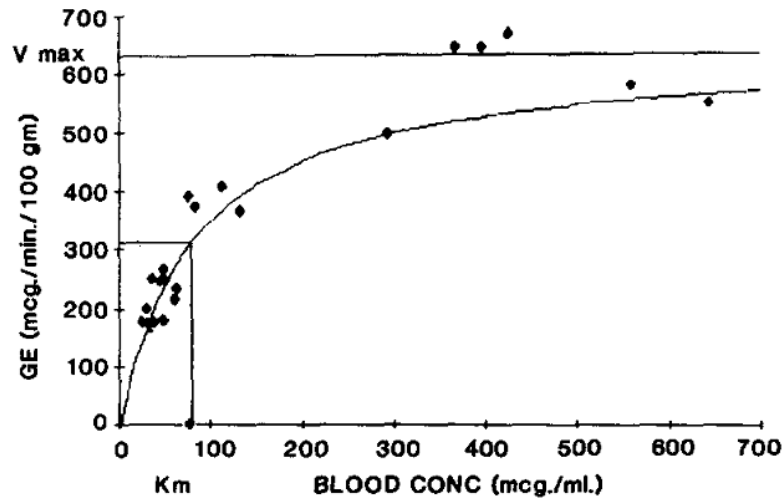


FIG. 1. Galactose elimination kinetics. Points represent individual animals. Superimposed line as determined by the Michaelis-Menten equation using the elimination constants, V_{max} and K_m , from Fig. 2.

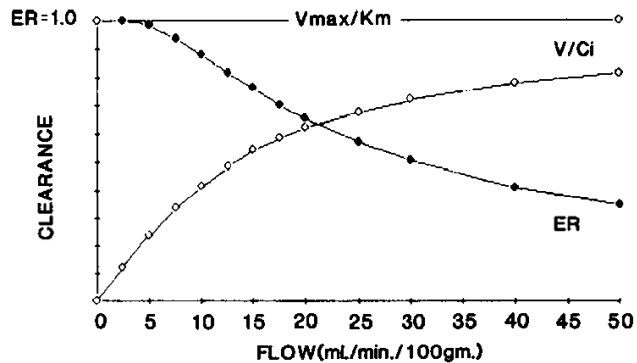
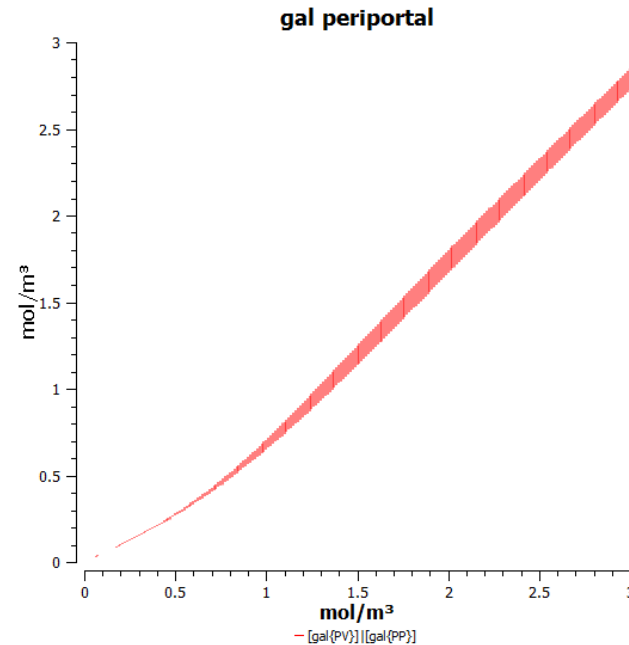


FIG. 6. Clearance and extraction ratio vs flow. Extraction ratio decreases as flow increases. Clearance increases with flow to a maximum of V_{max}/K_m .



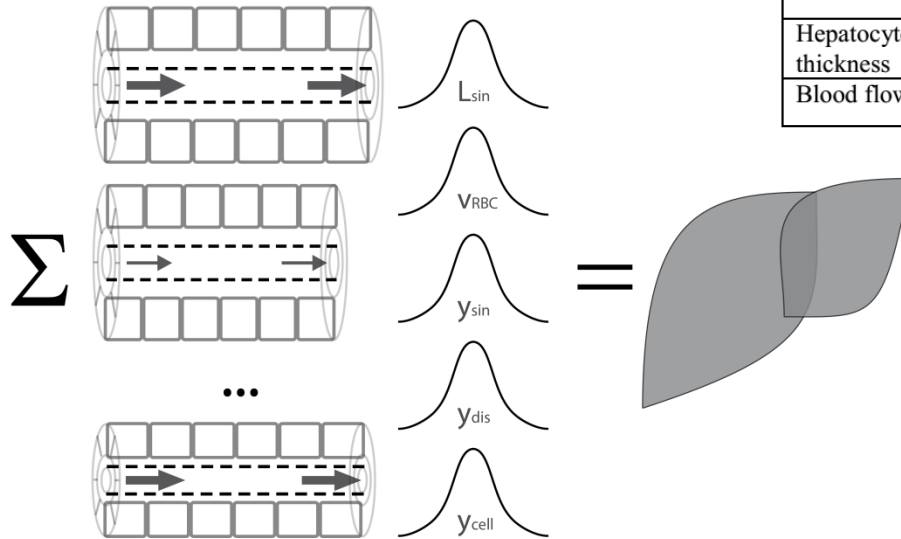
TODO: Improving Integration Times

- generation of optimized C++ code for solver

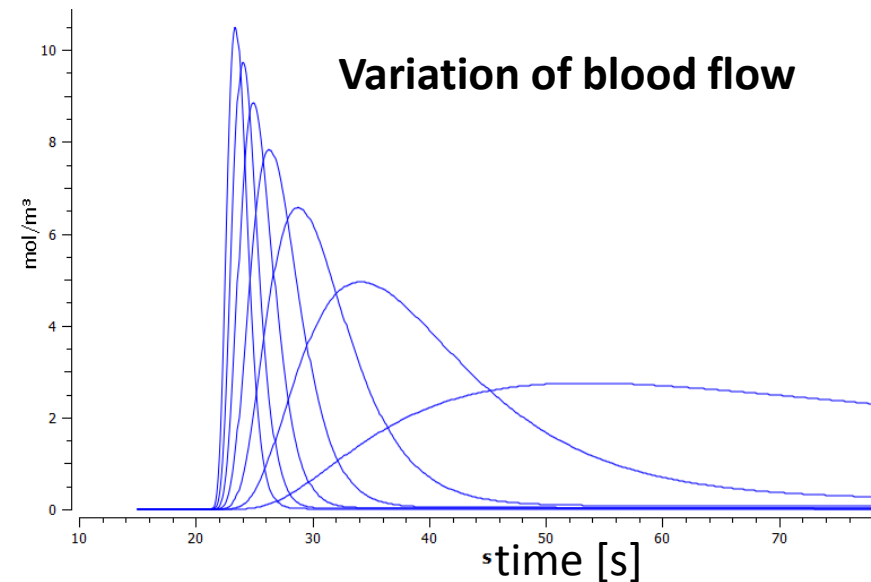
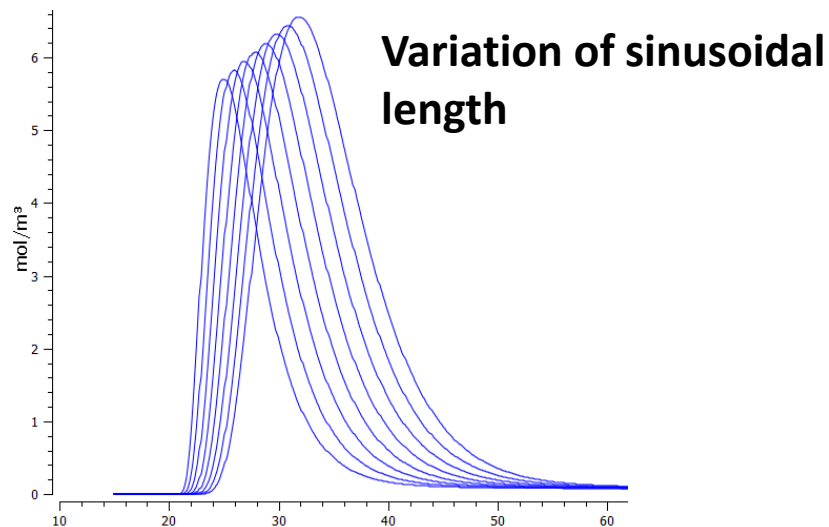
**ORGAN-SCALE –
WHOLE LIVER METABOLISM**

ORGAN-SCALE

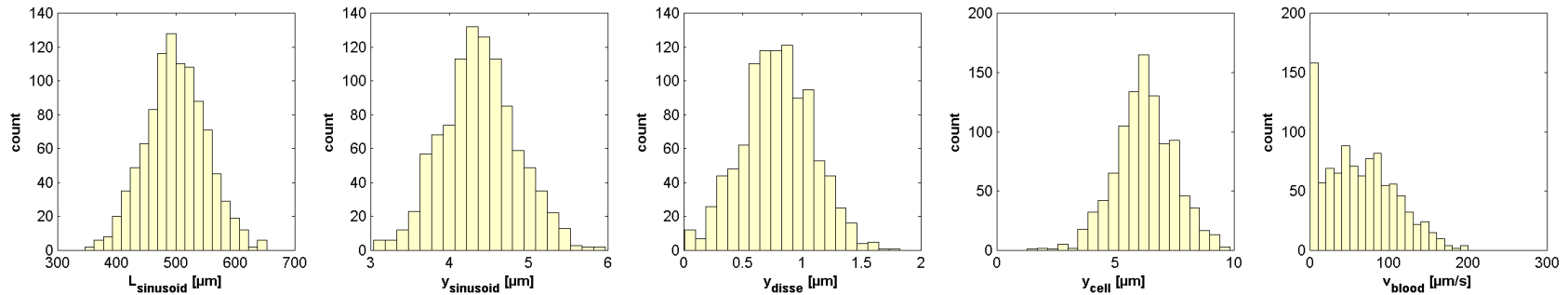
Parameter		mean μ	standard deviation σ
Sinusoidal length	L_{\sin}	500 μm	70 μm
Sinusoidal radius	y_{\sin}	4.4 μm	0.45 μm
Width of Disse space	y_{dis}	0.8 μm	0.3 μm
Hepatocyte sheet thickness	y_{cell}	1/4*25 μm	1/4*5 μm
Blood flow velocity	v_{RBC}	60 $\mu\text{m/s}$	50 $\mu\text{m/s}$



- whole liver modelled by integrating heterogeneous contribution of sinusoidal units differing in blood-flow and tissue-architecture



WORK IN PROGRESS



- Calculation of distributions of sinusoidal units
 - optimized C++ integration routines
 - parallelization & integration
- Simulations of alterations
 - **Galactosemias**
 - **homogeneous**
 - changes in GEC during aging
 - changes in GEC during CCL4 intoxication
 - changes in GEC during
 - **heterogeneous**
 - local perfusion inhomogeneities

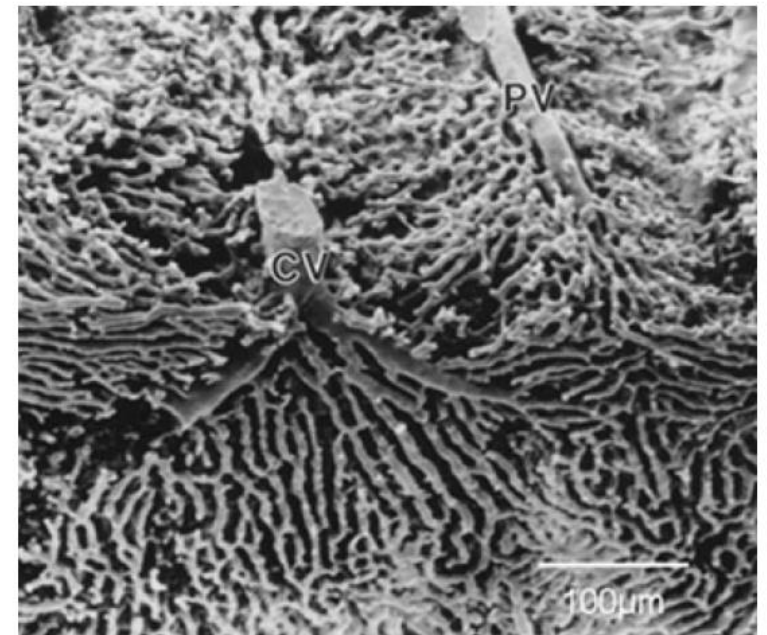
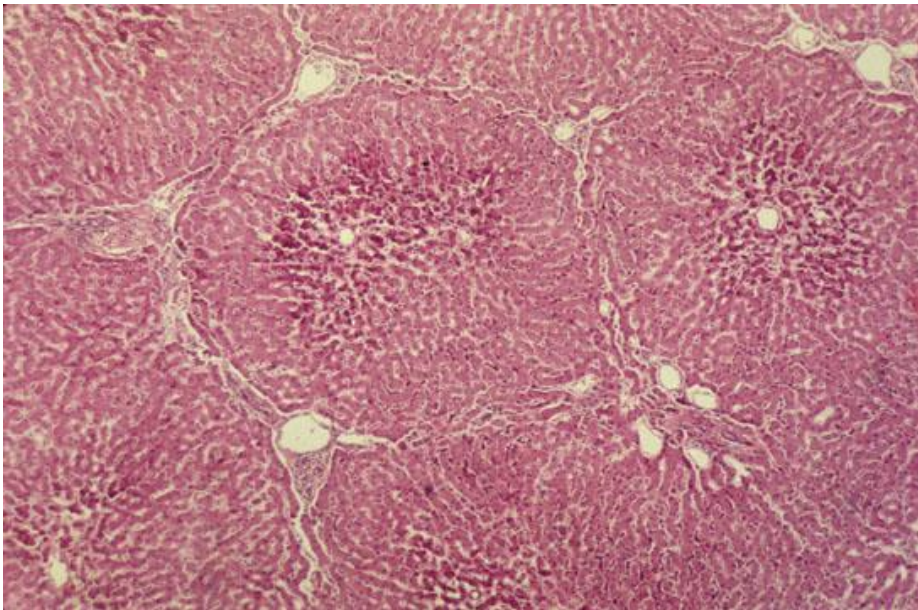


Fig. 2. Vascular cast of the hepatic microvasculature illustrating the tortuous, anastomotic sinusoids adjacent to the portal venule (PV) and the more parallel and larger sinusoids near the central venule (CV) (McCuskey, 1993).

SINUSOID

- principal vessels for exchange between blood and hepatocytes
- ~ 6-8µm diameter
- periportal sinusoids are narrower and more tortuous than the wider and straighter central ones
- Sinusoid network is heterogeneous
 - **near portal vein** arranged as **interconnecting polygonal networks**
 - farther away from portal vein organized as **parallel vessels terminating in the central vein**
 - short **intersinusoidal sinusoids** connect adjacent parallel sinusoids

Scanning electron micrograph showing fenestrated sinusoids and hepatocytes in a mouse liver.

http://www.easloffice.eu/jhep/contest/website/see_photos.html

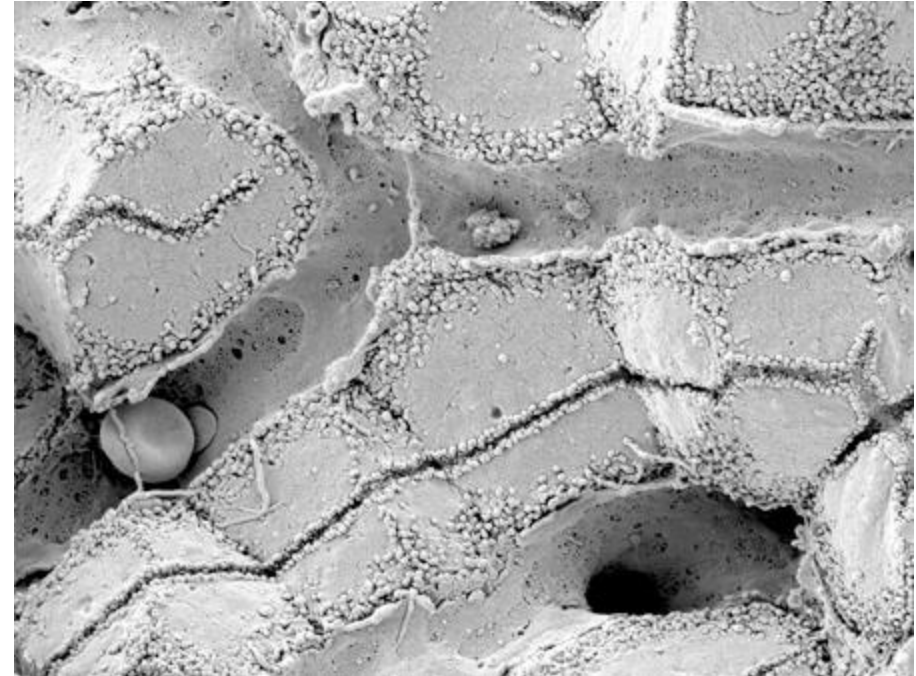


TABLE 1. COMPARISON OF MEASUREMENTS ON SINUSOIDS AND BLOOD CELLS IN MICRONS ± S.E.

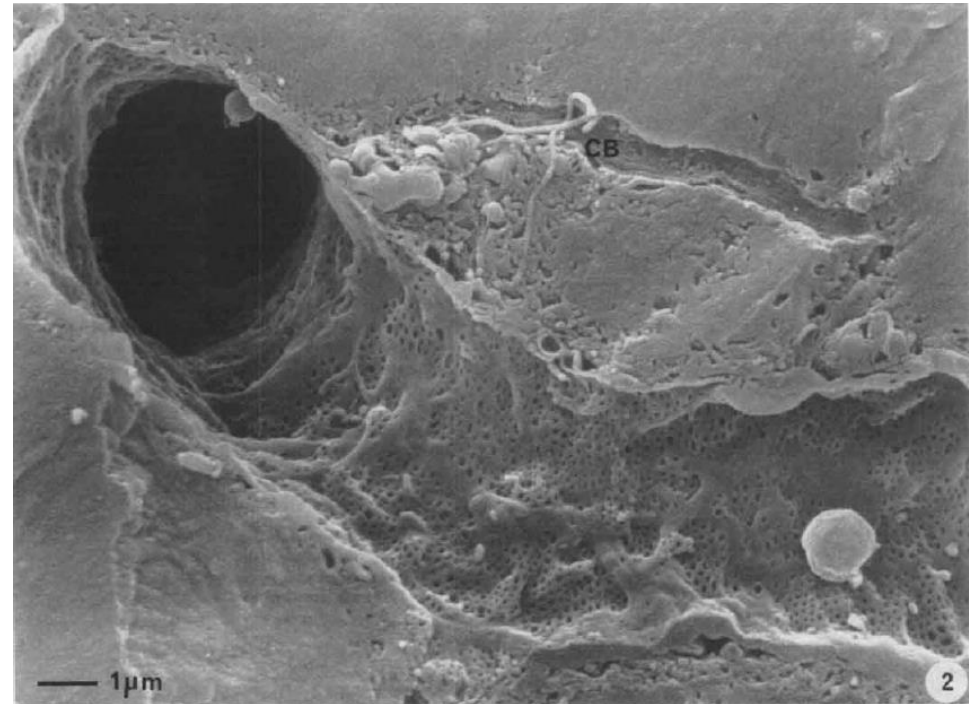
	<i>In vivo</i> /LM*	In plastic/LM	After CPD/SEM
Portal sinusoid	5.9 ± 0.17 (n = 545, 6 rats)	6.42 ± 0.12 (n = 696, 2 rats)	4.09 ± 0.06 (n = 1, 452, 10 rats)
Central sinusoid	7.1 ± 0.29 (n = 498, 6 rats)	7.62 ± ND ^b (n = 696, 2 rats)	5.67 ± ND (n = 1, 452, 10 rats)

Scanning electron microscope observations on the structure of portal veins, sinusoids and central veins in rat liver. Wisse, E.; De Zanger, R. B.; Jacobs, R. & McCuskey, R. S.; *Scan Electron Microsc*, **1983**, 1441-1452

The liver sieve: considerations concerning the structure and function of endothelial fenestrae, the sinusoidal wall and the space of Disse. Wisse, E.; De Zanger, R. B.; Charels, K.; Van Der Smissen, P. & McCuskey, R. S. *Hepatology*, **1985**, 5, 683-692

ENDOTHELIAL FENESTRAE

- liver sinusoids unique capillaries
 - **open pores (fenestrae)** in sinusoidal wall
 - **lack basal membrane** underneath endothelium
- fenestrae act as sieving barrier between blood and hepatocytes
 - morphological & physiological evidence that fenestrae act as a **dynamic filter**
 - important role in lipid metabolism (namely **chylomicrons**)
- Liver sinusoidal endothelial cells (**LSEC**) constitute sinusoidal wall
 - numerous endocytotic vesicles
 - effective uptake of a wide variety of substances from blood via receptor-mediated endocytosis (Braet, 2004)
 - transcytosis transport across the endothelium to surrounding tissue
 - scavenger system



Contribution of high-resolution correlative imaging techniques in the study of the liver sieve in three-dimensions. Braet, F. et al; *Microsc Res Tech*, **2007**, 70, 230-242
Structural and functional aspects of liver sinusoidal endothelial cell fenestrae: a review. *Comp Hepatol*, Braet, F. & Wisse, E., **2002**, 1, 1
The liver sieve: considerations concerning the structure and function of endothelial fenestrae, the sinusoidal wall and the space of Disse. Wisse, E.; De Zanger, R. B.; Charels, K.; Van Der Smissen, P. & McCuskey, R. S. *Hepatology*, **1985**, 5, 683-692

FENESTRAE

- diameter ~**50-200nm**
- ultrastructure same across species
 - groups of fenestrae arranged in so called **sieve plates**
- differences periportal & perivenous
 - diameter decreases (110.7 to 104.8nm)
 - frequency increases (9 to 13 per μm^2)
 - increased porosity from pp to pv from 6 to 8%
- number and diameter may vary between individuals & within single individual under various physiological and pharmacological circumstances

Scanning electron micrograph of hepatocyte microvilli protruding through the sinusoidal endothelial cell fenestrations.

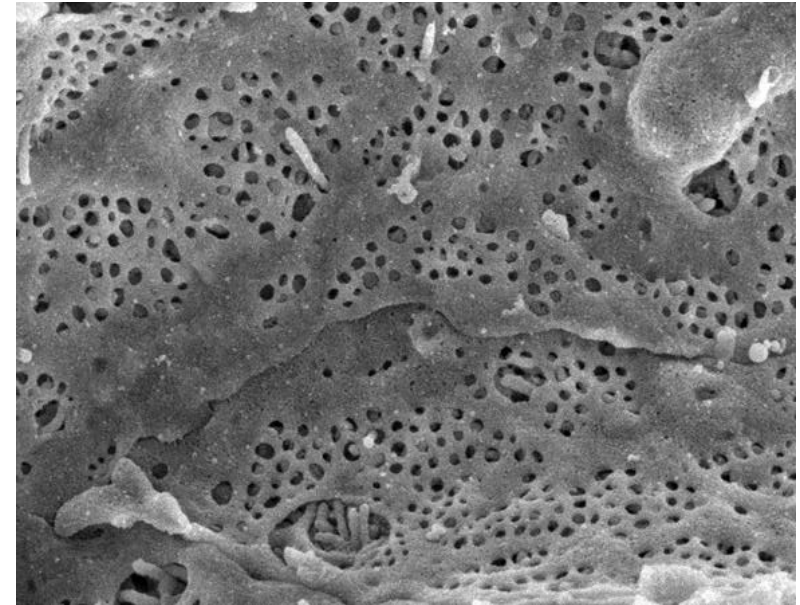
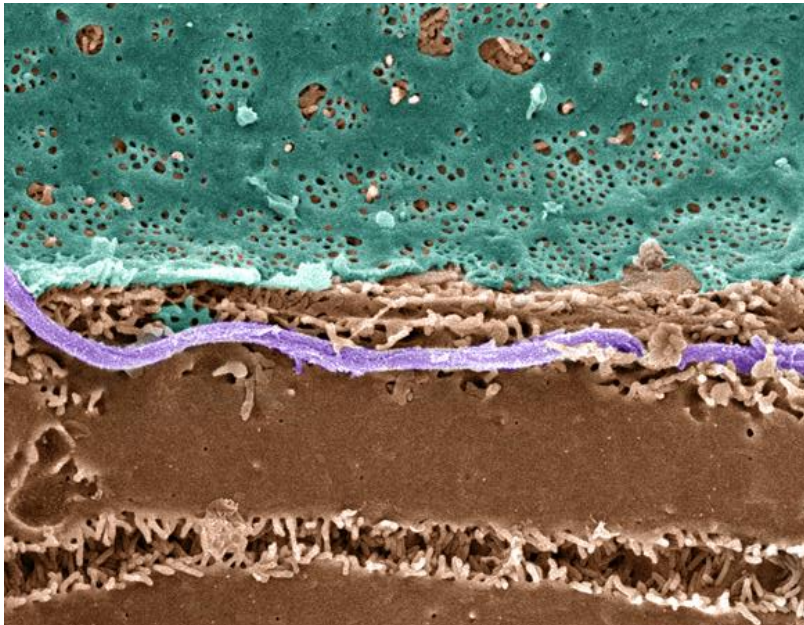


Table 1: Fenestration pattern in different species Brief overview of fenestrae characteristics of different species. Notice the large variations in diameter and number of fenestrae between the different species. The reported data from this table were obtained by at random measurements along the sinusoids. "n.d." = no data available. Data are expressed as mean \pm S.D. In case of baboon, human and rainbow trout the data correspond with the minimum and maximum diameter or number of fenestrae measured.

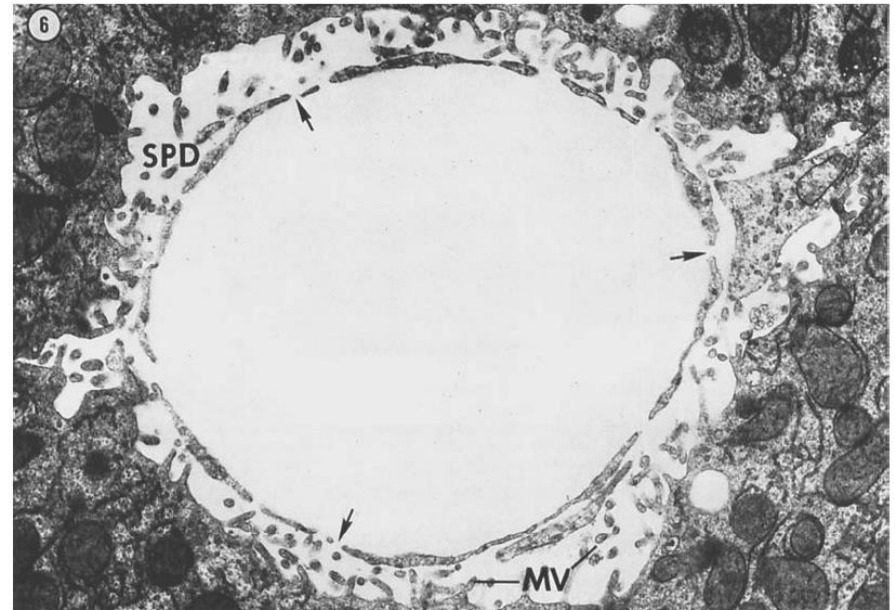
Species (ref.)	Diameter (nm)	Number of fenestrae / μm^2
Rat [25]	98.0 ± 13.0	20.0 ± 6.3
Mouse [26]	99.0 ± 18.0	14.0 ± 5.0
Rabbit [27]	59.4 ± 4.8	17.3 ± 3.8
Chicken [23]	89.6 ± 17.8	2.9 ± 0.3
Baboon [20]	92 – 116	1.4 – 1.9
Human [28]	50 – 300	15 – 25

SPACE OF DISSÉ



Pseudo-colored Scanning EM of an hepatic plate, accentuating the **fenestrated sinusoidal endothelium (blue)**, **hepatocyte (brown)** and a **collagen fibril (lavender)**.

Hepatocytes surface enlarged via **microvilli**.



6 Intermediate sinusoid. The lining cells possess fenestrations (arrows) and there is no basement membrane. The space of Dissé (SPD) is voluminous. The surface of the parenchymal cells is characterized by numerous microvillae (MV). The blood plasma has free access to the liver cells. Glutaraldehyde; OsO₄; Epon; 13,500 ×.

The fine structure of rat liver sinusoids, space of Dissé and associated tissue space.

Burkel, W. E. & Low, F. N.; *Am J Anat*, 1966, 118, 769-783

http://www.easloffice.eu/jhep/context/website/see_photos.html

SINUSOID ULTRASTRUCTURE

- fenestration & absence of basement membranes provide direct access of blood plasma to hepatocytes

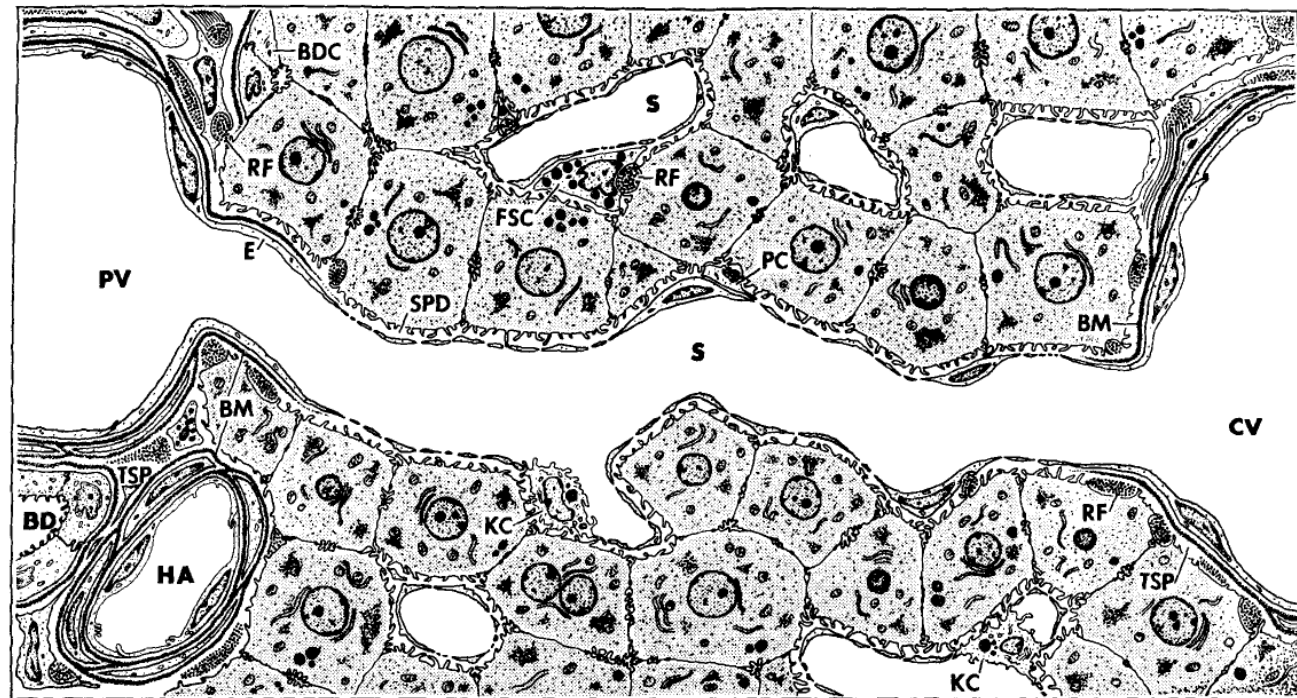


Fig. 1 *Fine structure in the rat liver lobule.* The periphery of the lobule is at the left where branches of portal vein (PV) hepatic artery (HA) and bile duct (BD) lie in the tissue space (TSP). Above, bile duct cells (BDC) abut on liver cells. The sinusoid (S) connects the portal vein with the central vein (CV). In the peripheral portion of the sinusoid both the endothelium (E) and its basement (boundary) membrane (BM) are continuous with those of the portal vein. In the intermediate portion the lining is fenestrated and there is no basement membrane. Centrally the cellular lining is continuous with the endothelium of the central vein and a basement membrane is present. Reticular fibers (RF) are found in the tissue space and in the space of Dissé (SPD) which surrounds the sinusoids. In places the sinusoids are lined by the cells of von Kupffer (KC). Perisinusoidal cells (PC) and fat storage cells (FSC) are in the space of Dissé. See text for interpretation.

TIGHT SINUSOIDS

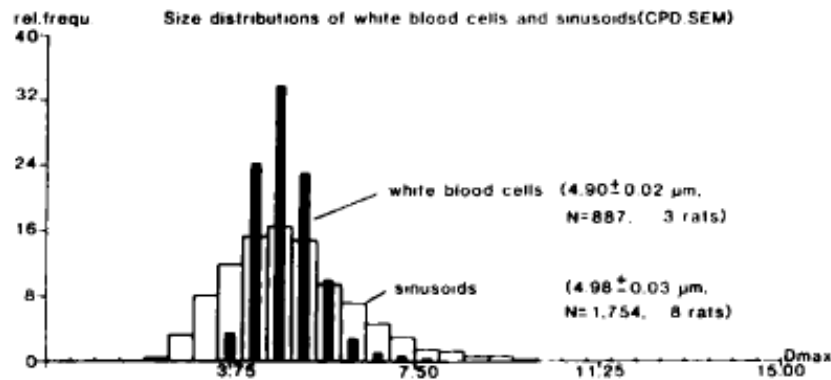
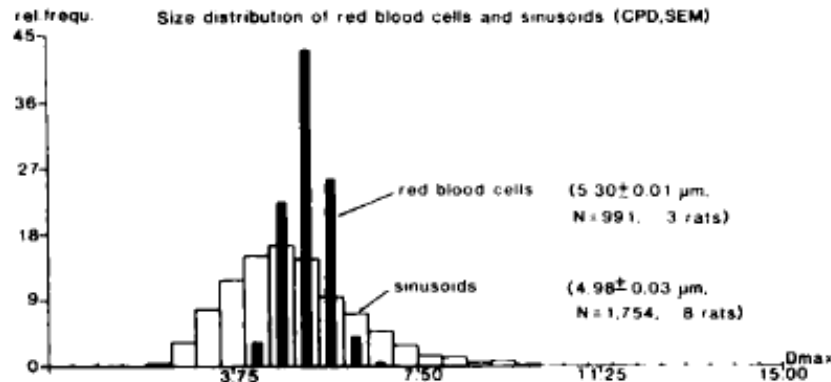


FIG. 9. Size distribution of sinusoids and red and white blood cells, extending the data of Table 1. From these two graphs, one might conclude that starting at $3.75 \mu\text{m}$ blood cells are larger than a certain percentage of sinusoids. At about the size of $7 \mu\text{m}$, white blood cells are bigger than most sinusoids, and these cells will progressively plug sinusoids in the range of approximately $4 \mu\text{m}$ (in SEM preparations).

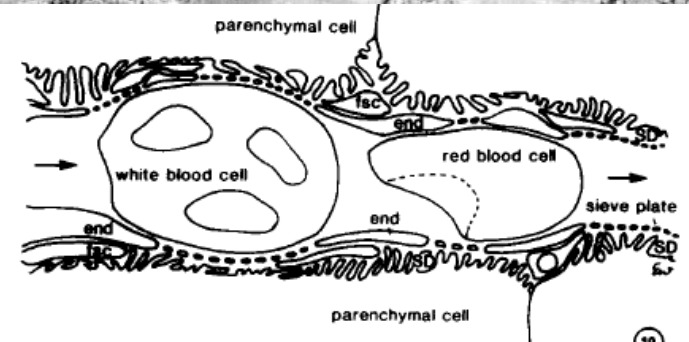
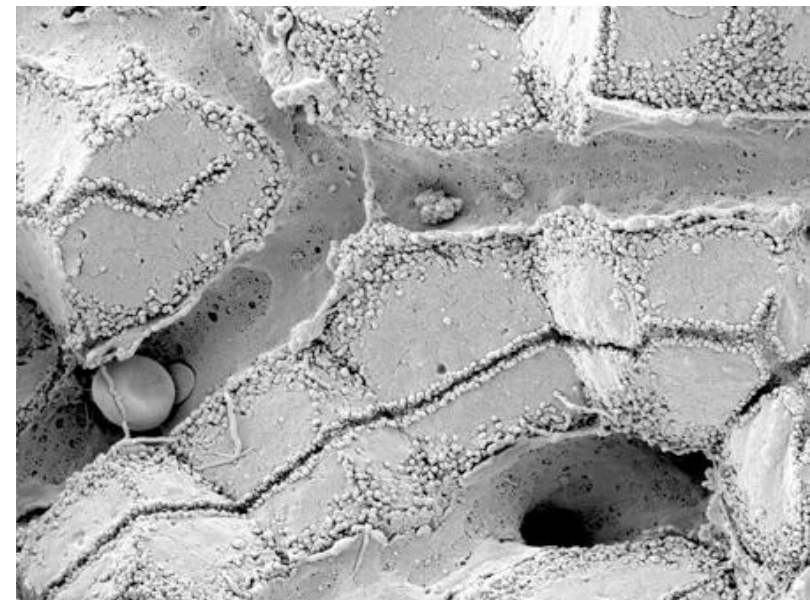


FIG. 10. shows the interaction of blood cells and the fenestrated sinusoidal wall. As observed in the *in vivo* microscope, red blood cells pass by in a single row and show typical deformation morphology. Their observed flexibility is enormous, and in slow streaming sinusoids one observes that red blood cells adapt their diameter constantly to the diameter of the sinusoid by expanding and narrowing. This implies that uptake and exchange is taking place from volumes of plasma in between the red blood cells. White blood cells are much more rigid than red blood cells and are thought to compress the space of Disse, thereby performing endothelial massage (Fig. 12).

BLOOD FLOW

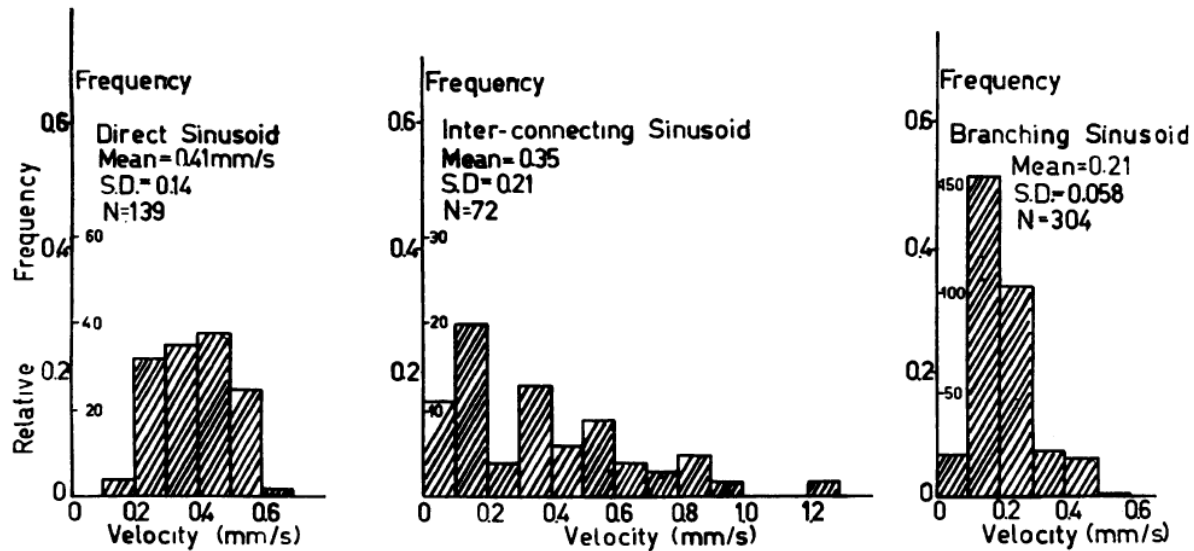


FIG. 1. Frequency distribution of the velocity of the erythrocytes in the direct sinusoids, the branching sinusoids and the interconnecting sinusoids.

The terminal hepatic microcirculation in the rat.

Koo, A.; Liang, I. Y. & Cheng, K. K.; *Q J Exp Physiol Cogn Med Sci*, **1975**, 60, 261-266

Intermittence of blood flow in liver sinusoids, studied by high-resolution in vivo microscopy. MacPhee, P. J.; Schmidt, E. E. & Groom, A. C.; **1995**, 269, G692-G698

BLOOD FLOW

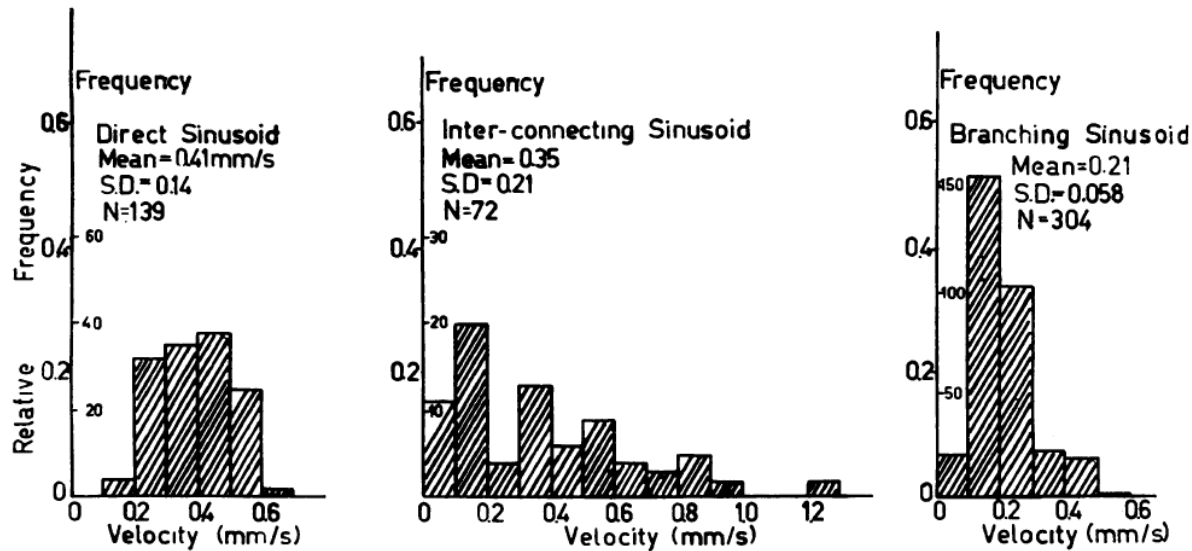


FIG. 1. Frequency distribution of the velocity of the erythrocytes in the direct sinusoids, the branching sinusoids and the interconnecting sinusoids.

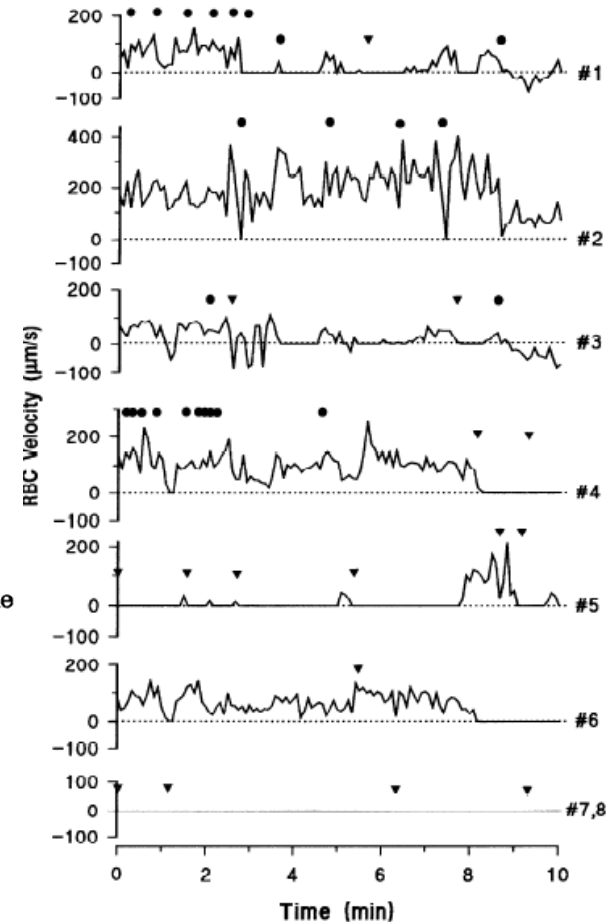
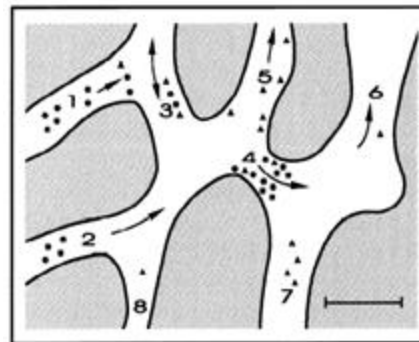


Fig. 3. Temporal overview of RBC velocity fluctuations over a 10-min period, in sinusoidal network from zone 1 of mouse liver (shown in Fig. 2). Measurements in each sinusoid were made every 5 s. Changes of flow in one sinusoid often produced changes in others. Instants are indicated at which a migrating Kupffer cell obstructed flow (●) or a circulating leukocyte slowed or stopped temporarily (▼). Sinusoids 7 and 8 had no flow throughout the 10-min period. Kupffer cells are seen in sinusoid 7, and in sinusoid 8 one Kupffer cell blocked flow throughout.



The terminal hepatic microcirculation in the rat.

Koo, A.; Liang, I. Y. & Cheng, K. K.; *Q J Exp Physiol Cogn Med Sci*, **1975**, *60*, 261-266
Intermittence of blood flow in liver sinusoids, studied by high-resolution in vivo microscopy. MacPhee, P. J.; Schmidt, E. E. & Groom, A. C.; **1995**, *269*, G692-G698

LYMPH

- substantial amount of hepatic lymph is generated in space of Dissé
 - space of Dissé is continuous with the tissue space at both ends of the sinusoid !
 - high protein content of hepatic lymph
- **lymphatic vessels** originate as blind-ending capillaries in the connective tissue spaces (portal tracts) associated with the portal veins and hepatic arteries
 - fluid contained in these lymphatics flows toward the **hepatic hilus** and eventually into the **cisternae chyli**

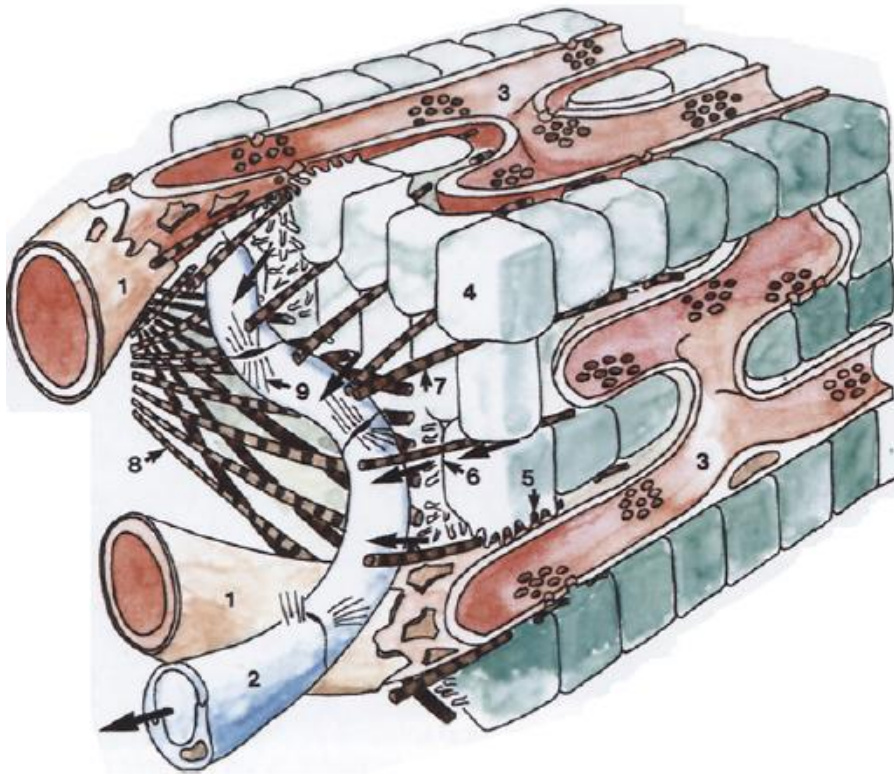


Fig. 5. Terminal lymphatics of the periportal area. The *thick arrows* indicate the possible lymph flow, coming from the space of Disse and entering a terminal lymphatic. The continuity between the space of Disse and the periportal area is represented by collagen fibers. 1, blood capillary entering the liver parenchyma; 2, terminal lymph vessel; 3, sinusoid; 4, periportal hepatocyte; 5, space of Disse; 6, space of Mall; 7, collagen fibers entering the limiting plate; 8, network of periportal collagen fibers; 9, anchoring filaments

Lymph circulation in the liver.

Ohtani, O. & Ohtani, Y.; *Anat Rec*; **2008**, 291, 643-652

The lymphatics of the liver.

Trutmann, M. & Sasse, D. ; *Anat Embryol (Berl)*, **1994**, 190, 201-209